

## Vertical Distribution of Dimethylsulfide, Sulfur Dioxide, Aerosol Ions, and Radon over the Northeast Pacific Ocean

M. O. ANDREAЕ\*, H. BERRESHEIM\*\*, T. W. ANDREAЕ\*

*Department of Oceanography, Florida State University, Tallahassee, FL 32306, U.S.A.*

M. A. KRITZ

*Atmospheric Sciences Research Center, State University of New York, Albany, NY 12222, U.S.A.*

T. S. BATES

*Pacific Marine Environmental Laboratory, National Oceanic and Atmospheric Administration, Seattle, WA 98115, U.S.A.*

and

J. T. MERRILL

*Graduate School of Oceanography, University of Rhode Island, Kingston, RI 02881, U.S.A.*

(Received: 22 August 1986; in revised form: 20 January 1987)

**Abstract.** Dimethylsulfide (DMS), sulfur dioxide ( $\text{SO}_2$ ), methanesulfonate (MSA), nonsea-salt sulfate ( $\text{nss-SO}_4^{2-}$ ), sodium ( $\text{Na}^+$ ), ammonium ( $\text{NH}_4^+$ ), and nitrate ( $\text{NO}_3^-$ ) were determined in samples collected by aircraft over the open ocean in postfrontal maritime air masses off the northwest coast of the United States (3–12 May 1985). Measurements of radon daughter concentrations and isentropic trajectory calculations suggested that these air masses had been over the Pacific for 4–8 days since leaving the Asian continent. The DMS and MSA profiles showed very similar structures, with typical concentrations of 0.3–1.2 and 0.25–0.31  $\text{nmol m}^{-3}$  (STP) respectively in the mixed layer, decreasing to 0.01–0.12 and 0.03–0.13  $\text{nmol m}^{-3}$  (STP) at 3.6 km. These low atmospheric DMS concentrations are consistent with low levels of DMS measured in the surface waters of the northeastern Pacific during the study period.

The atmospheric  $\text{SO}_2$  concentrations always increased with altitude from <0.16–0.25 to 0.44–1.31  $\text{nmol m}^{-3}$  (STP). The nonsea-salt sulfate ( $\text{nss-SO}_4^{2-}$ ) concentrations decreased with altitude in the boundary layer and increased again in the free troposphere. These data suggest that, at least under the conditions prevailing during our flights, the production of  $\text{SO}_2$  and  $\text{nss-SO}_4^{2-}$  from DMS oxidation was significant only within the boundary layer and that transport from Asia dominated the sulfur cycle in the free troposphere. The existence of a 'sea-salt inversion layer' was reflected in the profiles of those aerosol components, e.g.,  $\text{Na}^+$  and  $\text{NO}_3^-$ , which were predominantly present as coarse particles. Our results show that long-range transport at mid-tropospheric levels plays an important role in determining the chemical composition of the atmosphere even in apparently 'remote' northern hemispheric regions.

**Key words.** Marine atmosphere, seawater, dimethylsulfide, sulfur dioxide, methanesulfonate, nonsea-salt sulfate, marine aerosol, radon, vertical distributions.

\* Present address: Max-Planck-Institut für Chemie, Postfach 3060, D-6500 Mainz, FRG.

\*\* Present address: School of Geophysical Sciences, Georgia Institute of Technology, Atlanta, GA 30332, U.S.A.

## 1. Introduction

The emission of biogenic dimethylsulfide ( $(\text{CH}_3)_2\text{S}$ , DMS) from the oceans to the atmosphere has been documented as a major natural source in the atmospheric sulfur budget, with an estimated global flux of about  $40 \text{ Tg S yr}^{-1}$  (Andreae and Raemdonck, 1983; Andreae, 1985, 1986 and references therein). Laboratory experiments have shown that DMS is an important precursor for sulfur dioxide ( $\text{SO}_2$ ) and methanesulfonic acid ( $\text{CH}_3\text{SO}_2(\text{OH})$ , MSA) due to its reaction with the hydroxy radical ( $\text{OH}$ ) during the day and the nitrate radical ( $\text{NO}_3$ ) at night (Wine *et al.*, 1981; Niki *et al.*, 1983; Atkinson *et al.*, 1984; Grosjean, 1984; MacLeod *et al.*, 1984; Winer *et al.*, 1984; Hatakeyama *et al.*, 1985). DMS contributes indirectly to the nonsea-salt sulfate ( $\text{nss-SO}_4^{2-}$ ) concentration in the marine atmosphere via further oxidation of  $\text{SO}_2$  to sulfate. Due to its low vapor pressure, MSA is presumed to be present mainly in the aerosol phase (Saltzman *et al.*, 1984), and gaseous MSA has not yet been identified in the atmosphere. (In this paper, we use MSA as abbreviation for both methanesulfonic acid, and methanesulfonate, the ionic form present in aerosols and precipitation.) In the marine aerosol MSA has been found at levels of about 6–7% by mole of the  $\text{nss-SO}_4^{2-}$  concentration (Saltzman *et al.*, 1983, 1985, 1986; Ayers *et al.*, 1986).

The distribution of DMS in the marine boundary layer at ground level has been studied extensively and a 0-dimensional chemical model has been successfully used to explain the observed concentrations and their diurnal behavior (Andreae *et al.*, 1985). Corresponding aircraft measurements have only recently been reported in two studies (Van Valin and Luria, 1985; Ferek *et al.*, 1986) in which samples were collected over subtropical and tropical regions of the Atlantic Ocean. In this paper we present data on the vertical distributions of DMS,  $\text{SO}_2$ , radon, aerosol MSA, and other aerosol constituents in temperate latitudes over the northeast Pacific Ocean. Corresponding data of DMS concentrations determined in surface seawater are also included.

## 2. Experimental

### 2.1. Sampling Region and Flight Logistics

Six sampling flights were made in the NCAR King Air off the northwest U.S. coast during 3–12 May 1985 (Figure 1, Table I). During flights I–III samples were taken at six different altitudes between *ca.* 0.1 and 3.6 km. Flight IV was conducted immediately following flight III, to continue the vertical profile up to 6 km. All samples were taken under similar meteorological conditions: in uncontaminated marine air masses behind cold fronts moving over the open ocean. The main purpose of flights V and VI was to extend the measurements at one flight level each (0.45 and 3.0 km, respectively) over a larger geographic distance in order to obtain more information about the regional distribution of

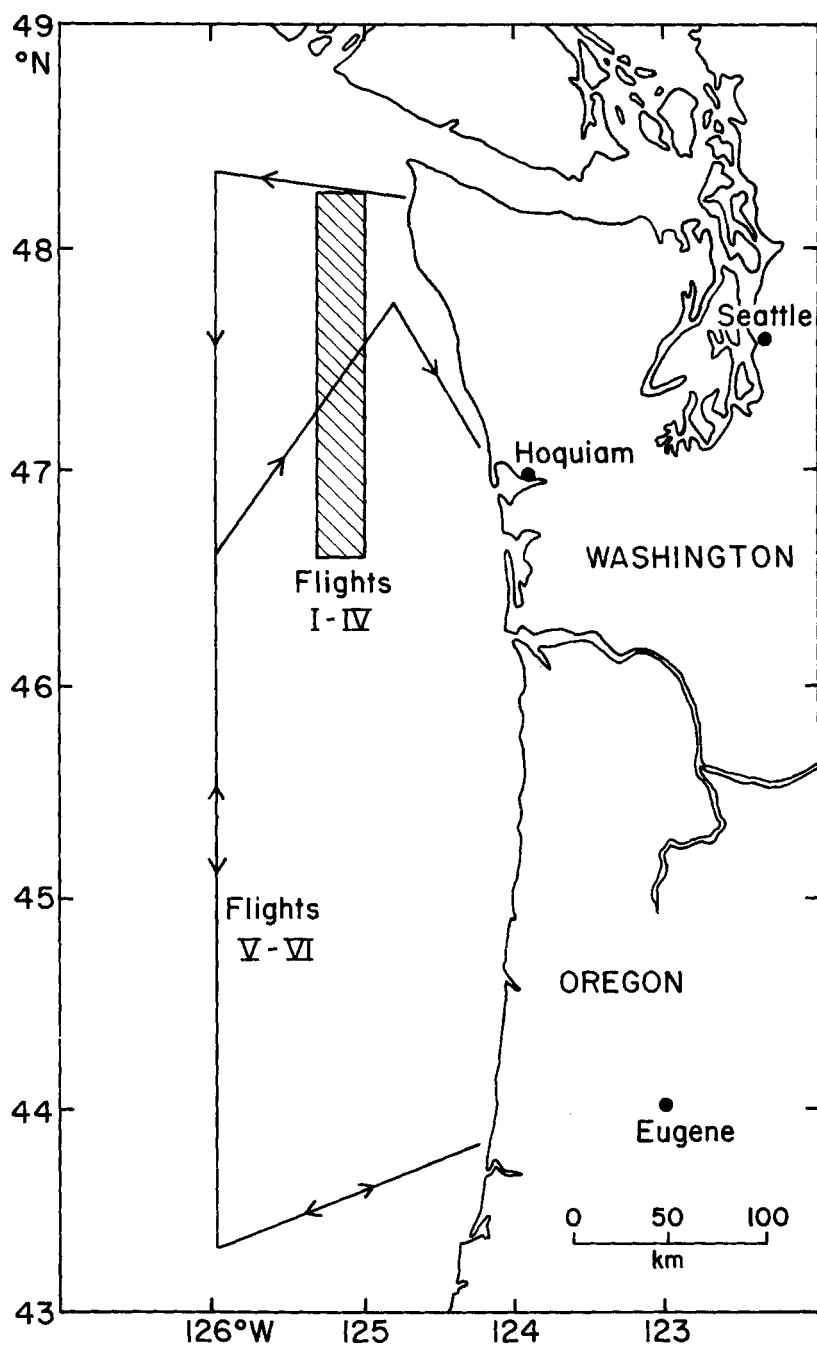


Fig. 1. Map of the study area. Sampling for Flights I-IV was conducted within the shaded area along north-south traverses at constant altitudes.

Table I. Flight dates and times during which sampling was conducted

Flight	Date (1985)	Time (PDT)
I	3 May	1034–1408
II	10 May	1502–1853
III	11 May	0836–1228
IV	11 May	1623–1957
V	12 May	1337–1644
VI	12 May	1815–2156

the individual species. Since these flights did not provide information which was significantly different from that obtained in the vertical profiles, they will not be discussed in detail here.

Seawater samples were collected aboard the R/V *McArthur* from 14–18 May 1985. The cruise track extended from the coast out 150 km off the northwest corner of Washington State. Vertical profiles of DMS, nutrients, chlorophyll, temperature, and salinity versus depth in the water column were obtained at several locations near the coast and at 25, 50, 100, and 150 km offshore. The rate of photosynthesis (productivity) was measured at two locations nearshore and at 150 km offshore.

## 2.2. Sampling and Analytical Methods

All concentrations except for radon are reported in units of nanomole per standard cubic meter ( $\text{nmol m}^{-3}$ ) or as parts per trillion by volume (pptv). Since our flowmeters are calibrated at 20 °C, standard conditions are assumed to be 101.3 kPa and 20 °C. At these conditions, one  $\text{nmol m}^{-3}$  corresponds to 24 pptv.

The techniques used for the sampling and determination of atmospheric DMS have been described in detail previously (Andreae *et al.*, 1985). Air was sampled from a Teflon manifold which was continuously flushed with outside air through Teflon tubing (8 mm i.d.) at a flow rate of about  $10 \text{ l min}^{-1}$ . The tubing was guided to the outside top of the aircraft through a stainless steel pipe with its inlet about 15 cm away from the surface. (The boundary layer thickness at the aircraft surface at our sampling station is less than 5 cm.) DMS was pre-concentrated by adsorption to gold wool contained in quartz glass tubes. Duplicate samples were collected simultaneously; the flow rate through each sampling tube was regulated to about  $2 \text{ l min}^{-1}$  and measured by integrating mass flowmeters (Teledyne Hastings-Raydist). The sampling time varied from 10 min in the mixed layer to about one hour at the highest flight levels. All samples were analyzed within 6 h after each flight. Previous studies had shown that the DMS on the gold surface is stable for at least 10 days if the samples are stored in the dark. The determination of DMS consisted of thermal desorption followed by cryogenic trapping, chromatographic separation, and flame photo-

metric detection (Andreae *et al.*, 1985). The precision and accuracy of this technique are about  $\pm 10\%$ , the detection limit near  $0.04 \text{ nmol m}^{-3}$  (1 pptv).

The determination of DMS in seawater has been described in detail elsewhere (Bates *et al.*, 1987); a brief summary is presented here. Seawater samples (15 ml) were purged with hydrogen to strip the volatile compounds, water vapor was removed from the gas stream by a trap at  $-30^\circ\text{C}$ , and the remaining gases were collected in a trap at liquid argon temperature. The trap was subsequently heated and the reduced sulfur gases separated with a fused silica capillary column (25 m length, 0.32 mm i.d., 5  $\mu\text{m}$  thick methylsilicone stationary phase equivalent to OV-1; Perkin-Elmer) and quantified with a flame photometric detector. Chlorophyll and productivity measurements were performed onboard using standard fluorometric and  $^{14}\text{C}$  techniques (Parsons *et al.*, 1984).

Aerosol samples were collected using an aluminum isokinetic nozzle which was designed to minimize sampling size bias in the intake system. Our intake design avoids distortion of the pressure field at the nozzle tip and the resulting problems associated with flow separation and turbulence (Figure 2). The profile of the nozzle leading edge follows the criteria for aircraft engine intakes at low Mach numbers (Küchemann and Weber, 1953). The opening angle inside the nozzle was kept below  $7^\circ$  to avoid flow separation. The nozzle was joined without gaps or sharp changes in diameter by a 2.5 cm i.d. aluminum tube to a ball valve inside the aircraft. In wind tunnel studies, this intake design has been shown to be much more efficient at collecting coarse aerosol particles than isokinetic inlets with sharp leading edges (A.C. Delany, pers. comm., 1985). The ball valve was immediately followed by a 3-stage filter unit enclosed in a Delrin filter holder. The sample flow rate was measured by a volumetric flowmeter (Vol-O-Flo, National Instrument Laboratories); the average flow rate was *ca.*  $15 \text{ m}^3 \text{ (STP) h}^{-1}$ . Depending on the flight altitude the sampling time varied between 30 min and one hour (longer sampling times are required at higher altitudes due to the decreased pumping efficiency at reduced ambient pressures).

The filter unit consisted of an exchangeable cassette holding three sequential 90-mm diameter filters on polyethylene supports. The aerosol was collected and

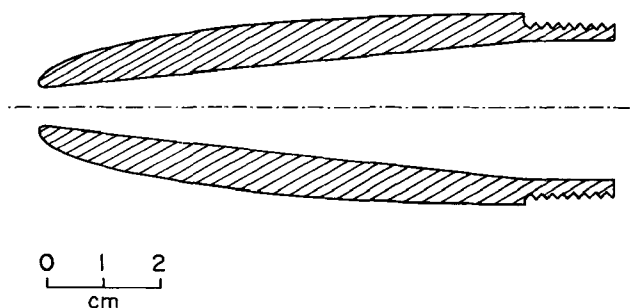


Fig. 2. Cross-section of the isokinetic intake nozzle used in the sampling system.

separated into coarse ( $> 1.5 \mu\text{m}$  diameter) and fine particles on the first two filter stages, consisting of a Nuclepore filter (nominal pore size  $8.0 \mu\text{m}$ ; 50% cut-off diameter at the face velocity used: *ca.*  $1.5 \mu\text{m}$ , John *et al.*, 1983) and a Zefluor filter (Membrana, nominal pore size  $1.0 \mu\text{m}$ ), respectively. The efficiency of the particle size separation by this stacked-filter arrangement is documented by the fact that almost all of the sea-salt component is found on the first stage (see Section 3.4 below). In laboratory studies, we have shown that the Nuclepore filters do not absorb significant amounts of  $\text{HNO}_3$  from ambient air (Talbot *et al.*, 1987). The third stage was a fast-flow cellulose filter (Schleicher and Schuell, FF# 2) impregnated with  $\text{K}_2\text{CO}_3$ /glycerol to trap  $\text{SO}_2$ . The preparation, storage, and blank behavior of the impregnated filters has been described in detail by Daum and Leahy (1983).

The filter samples were placed in polyethylene vials and extracted immediately after each flight. The aerosol filters were leached by ultrasonic treatment with 10 mL of deionized water. (The Zefluor filters were first soaked with 1 mL of methanol (Baker, spectrophotometric grade) to reduce their hydrophobic properties.) The solutions were then stored in a refrigerator for later analysis for major ion and MSA concentrations. The impregnated filters were first cut into halves, one of which was extracted with 10 mL of 0.06%  $\text{H}_2\text{O}_2$  whereby all sulfur (IV) species adsorbed on the filter were dissolved and converted to sulfate.

All filter samples were analyzed by ion chromatography (HPIC) on a Dionex 2020i ion chromatograph, using the AS4 and CS1 columns and standard eluents. For the determination of the sulfate concentration in the impregnated filter samples, the standard solutions were matched in their matrix composition to the sample solutions to compensate for the effect of the carbonate matrix on the retention time and height of the sulfate peaks. A 2.1 mM  $\text{NaHCO}_3$ /1.9 mM  $\text{Na}_2\text{CO}_3$  eluent was used in the analysis of these samples. The precision of the aerosol ion measurement is *ca.* 10%, with the largest uncertainties due to the filter blank corrections.

The aerosol MSA concentrations were determined using the AS4 column with a weak eluent (0.45 mM  $\text{NaHCO}_3$ ). Aqueous standards were prepared from methanesulfonic acid (Aldrich, 98%). The impregnated filter samples were diluted 1:100 with a  $\text{H}_2\text{O}/\text{CHCl}_3$  solution before analysis.

The collection efficiency and capacity of the impregnated filters for  $\text{SO}_2$  was studied in laboratory experiments. A standard concentration of  $22 \text{ nmol SO}_2 \text{ m}^{-3}$  was produced in a dynamic dilution system (Metronics Dynacalibrator 340) using a  $\text{SO}_2$  permeation device (Metronics, Dynacal). The same filter arrangement as used for field sampling was used for sampling from the calibration system, including Nuclepore and Zefluor filters, with the same face velocity and sampling times. The sulfate recovery was found to be quantitative within the analytical precision. The overall precision of this technique is 10–20%, with the uncertainty largely due to the blank correction required.

The radon concentration measurements were made using the active deposit method, in which the short-lived daughters of radon are collected on filters which are then analyzed immediately (Evans, 1955; Polian, 1972; Larson, 1973). The aerosol collection system consisted of an aerodynamically shaped inlet, the filter holder, a turbine flowmeter, and a variable speed pump. Large tubing diameters and bend radii were used to minimize aerosol and flow losses. In operation the pump speed was adjusted so that the collection was isokinetic, and was nominally 2 ambient cubic meters per minute. Particles were collected on the 11.4 cm central area of 15 cm diameter Whatman 541 filters. The nominal sampling time was 20 minutes, and was chosen to correspond to the sulfur species collection times. Following sampling, the filters were placed on a 7.25 cm diameter silicon detector. Each sample was counted for two (or more) successive tenminute periods, during which time the next sample was being collected.

Alpha rather than beta activity was monitored in these measurements, since alpha-based systems are significantly less sensitive to cosmic ray-induced background counts, which was an important factor for measurements at higher altitudes. The detector background count rate at 10 000 feet altitude was approximately 0.5 per min, which was always more than an order of magnitude below the radon daughter-derived count rates. Background count rates were monitored periodically during each flight. Radon concentrations for each sample were computed independently for each of the counting periods, and generally agreed within a few percent. (This also confirmed the assumption that the daughters were in equilibrium with the parent radon.) The system was calibrated using NBS traceable Americium-241 thin-source standards and calibrated filters. Overall measurement precision and accuracy were calculated to be  $\pm 10\%$  and  $\pm 20\%$ , respectively.

### 3. Results and Discussion

#### 3.1. *Meteorological Conditions and Air Mass Trajectories*

The meteorological conditions for flights I–IV are summarized in Figure 3. All three sampling days were dominated by westerly winds and atmospheric subsidence within one to two days following the passage of cold fronts. The potential temperature profiles show that conditions within the lower levels were almost neutral and became more stable at higher altitudes. This stable stratification was especially evident above 3 km on 11 May (Flights III and IV). Typical mixed layer thickness during our flights was up to 1 km, typical boundary layer thickness about 2–3 km. (We use the term ‘mixed layer’ to describe the layer of nearly constant potential temperature and composition below cloudbase, and the term ‘boundary layer’ to comprise both this layer and the overlying convective cloud layer.) The cloud base levels are clearly reflected by the maxima in

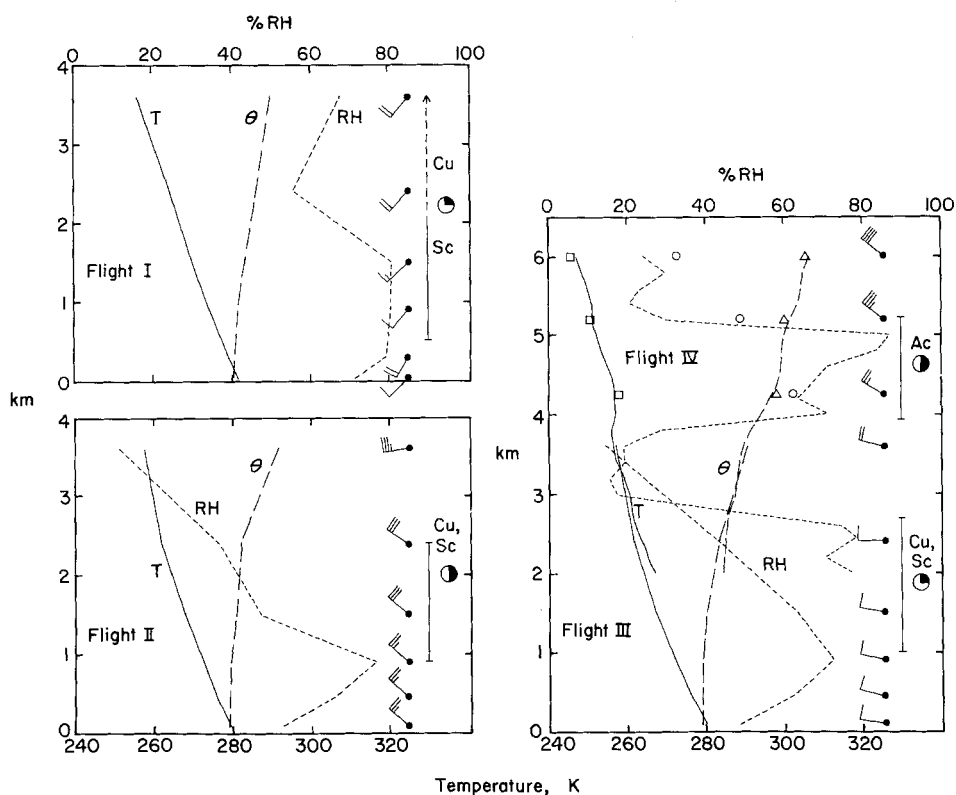


Fig. 3. Soundings of temperature ( $T$ ), potential temperature ( $\theta$ ), relative humidity ( $RH$ ), and winds determined during flights I to IV. For flights I–III the soundings are based on the mean values obtained during the horizontal sampling legs (the wind symbols indicate the elevations at which the data were collected). For flight IV the actual sounding obtained during the aircraft ascent is plotted together with symbols indicating the mean values at the sampling elevations.

the relative humidity profiles. Both the horizontal and vertical wind shear were insignificant, except for the highest flight levels above the cloud tops. In general the weather conditions were characterized by scattered cloudiness without significant precipitation. A few isolated showers of short duration were observed during flights I and II.

Figure 4 shows back-trajectories from the flight area. The trajectories are on isentropic surfaces labeled with the potential temperature value. The travel time shown varies from 4 to 12 days. The techniques and data sources used are like those described by Merrill *et al.* (1985). The vertical motion of the air parcels is shown in pressure coordinates in the upper panel of each part of the figure. The trajectories shown are representative examples from ensembles of trajectories for a grid of points surrounding the flight area. As discussed below, most of the trajectories show subsidence near the coast, i.e., gradual downward motion. Only for upper levels do the trajectories show contact with land (Korea, Soviet

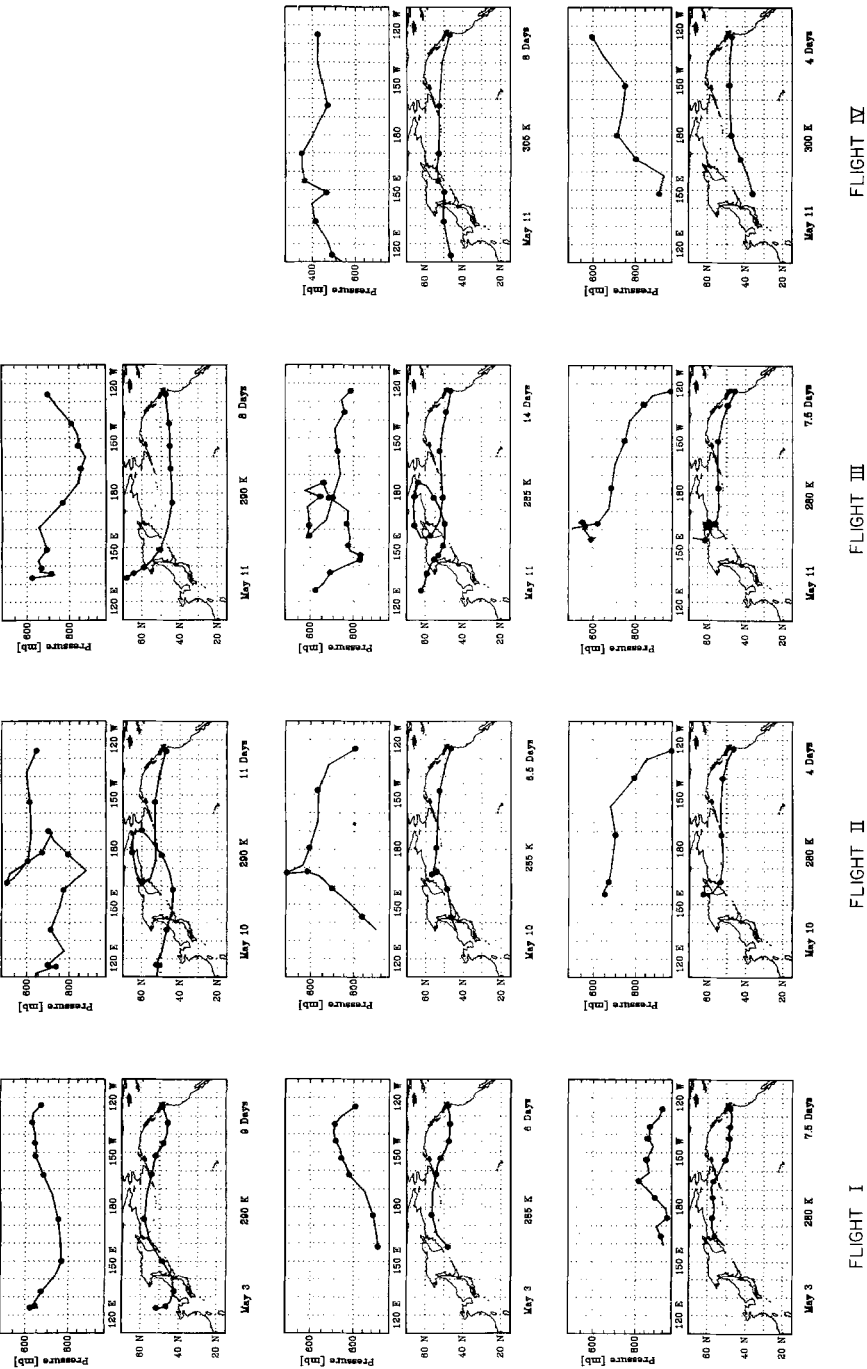


Fig. 4. Isentropic back-trajectories for flight I (3 May 85), flight II (10 May 85) and flights III and IV (11 May 85). The dots are at 24 h intervals. The potential temperature and the total time covered by each trajectory are indicated below each panel. Note that the 305 K trajectory on 11 May has a different pressure range.

Union, Northern China). All the trajectories at lower levels indicate that the air was in the marine boundary layer prior to its passage across the Pacific.

### 3.2. Radon

The vertical radon profiles from flights I, II, and III are shown in Figure 5. (Due to experimental problems no Rn data are available for flight IV.) The individual values all fall in the range 4–10 pCi m<sup>-3</sup> (STP) (9–22 dpm m<sup>-3</sup> (STP)). While these values are definitely marine, they are still an order of magnitude greater than those typical of truly remote marine situations (Wilkniss *et al.*, 1973) and thus suggest a residual continental influence.

Since essentially all of the radon in the atmosphere originates from the continental crust, the radon profiles and concentrations which were observed in

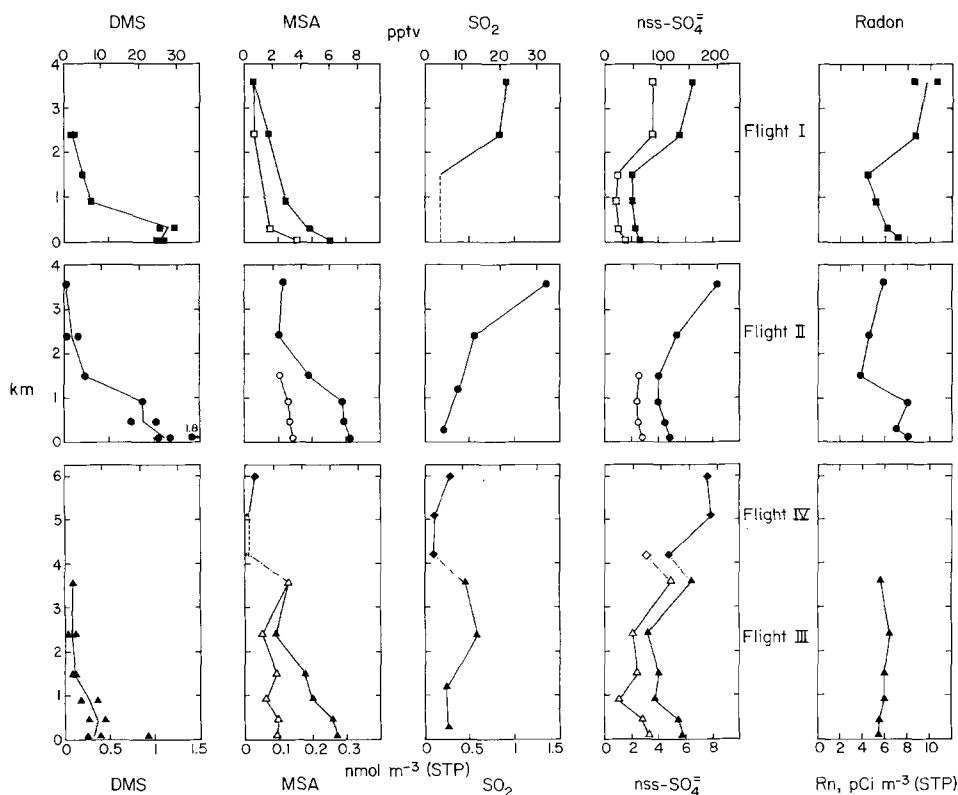


Fig. 5. Vertical distributions of dimethylsulfide (DMS), methanesulfonate aerosol (MSA), sulfur dioxide (SO<sub>2</sub>), nonsea-salt sulfate (nss-SO<sub>4</sub><sup>2-</sup>) and radon obtained over the northeastern Pacific during flights I-IV (3-11 May 1985). For the aerosol constituents, the open symbols represent the fraction below 1.5 μm diameter and the closed symbols the total concentration. Sulfur species concentrations are given in nmol m<sup>-3</sup> (STP) and as mixing ratios (pptv) (for condensed phase constituents, 'pptv' represents a molar mixing ratio, i.e., moles of substance per mole air).

the Eastern Pacific reflect both the original Rn concentration when the air mass in question left the Asian continent, and the radioactive decay which occurred during the oceanic transit. The mean radon profile typical of spring conditions over the central U.S. (Liu *et al.*, 1984) shows radon concentrations of ca.  $100\text{--}200\text{ pCi m}^{-3}$  in the boundary layer,  $20\text{--}60\text{ pCi m}^{-3}$  at 2 km, and relatively constant levels of  $10\text{--}20\text{ pCi m}^{-3}$  at 3–8 km. Assuming a similar radon distribution over Asia, we can examine our observed Rn profiles for consistency with predictions based on the isentropic trajectories. The air masses sampled above 2 km on flight I, at 3.6 km on flight II, and from the surface to 3.6 km on flight III all left Asia at 500–700 mbar (3–5.5 km) about 8 days before sampling. The original radon levels of  $10\text{--}30\text{ pCi m}^{-3}$  should have decreased by a factor of about 4 over this period (half life: 3.8 days) to about  $2.5\text{--}7.5\text{ pCi m}^{-3}$ . Figure 5 shows that the observed values are in excellent agreement with this prediction.

The Rn levels below 2 km on flight I cannot be easily interpreted, since the back-trajectories terminate at the sea surface off Eastern Asia, and suggest some pronounced vertical movement in their source region. On the other hand, the relatively high Rn concentrations in the lowest km during flight II are readily explained by the rapid transport of this air mass (*ca.* 4 days) from a level of 650 mbar (*ca.* 3.5 km) over Asia. The Rn data obtained here therefore lend strong support to the validity of the isentropic trajectory calculations. They suggest, in particular, that rapid transport (4–8 days) of free tropospheric air from Asia to the west coast of North America is typical for the conditions investigated here.

### 3.3. Sulfur Compounds

*Dimethylsulfide.* Figure 5 shows the vertical distribution of DMS as measured during flights I–III. Due to experimental problems, no reliable DMS data could be obtained at the 3600 m level in flight I or above this level (flight IV). The DMS concentrations close to sea level (30–90 m) varied between  $0.25$  and  $1.25\text{ nmol m}^{-3}$  (STP), relatively low values compared to those obtained in tropical and subtropical latitudes (average  $2\text{--}3\text{ nmol m}^{-3}$ ; Andreae and Raemdonck, 1983; Andreae *et al.*, 1985; Ferek *et al.*, 1986). Elevated concentrations of  $0.83$  and  $1.8\text{ nmol m}^{-3}$  were measured inshore at 90 m during the transit to the study area on flights II and III. Within the mixed layer, the DMS concentrations were constant within the limits of the analytical method and then decreased through the convective cloud layer to very low values within the free troposphere.

The concentrations of DMS in the mixed layer are consistent with the measurements in surface seawater: On the continental shelf (2–50 km offshore), DMS averaged  $2.2 \pm 0.6\text{ nmol l}^{-1}$  ( $n = 33$ ), while concentrations further offshore (100–150 km) were appreciably lower ( $0.8 \pm 0.2\text{ nmol l}^{-1}$ ,  $n = 4$ ). These concentrations are similar to those obtained during May 1983 (Bates and Cline, 1985) and suggest that DMS concentrations in the open Pacific Ocean were still at levels characteristic of the winter season (Bate *et al.*, 1987). Chlorophyll *a* con-

centrations offshore were  $0.2 \mu\text{g l}^{-1}$ , while on the continental shelf they ranged from  $4\text{--}17 \mu\text{g l}^{-1}$ . Productivity measurements were also an order of magnitude higher on the continental shelf ( $500 \text{ mg C m}^{-2} \text{ d}^{-1}$ ) than offshore. The higher biological activity on the shelf was probably due to the shallower depth of the aquatic mixed layer (20 vs. 44 m) which may have prevented the plankton from being vertically transported out of the photic zone.

The DMS concentration data can be used to estimate the flux of DMS from the ocean to the atmosphere using the surface renewal model (Holmén and Liss, 1984). Using an air-sea exchange coefficient of  $3 \text{ m d}^{-1}$  (Bates *et al.*, 1987; based on wind velocities of  $10 \text{ m s}^{-1}$  and surface seawater temperatures of  $9^\circ\text{C}$ ), the flux of DMS from the ocean to the atmosphere is about  $2 \mu\text{mol m}^{-2} \text{ d}^{-1}$ . This flux is about a factor of 3–4 lower than the DMS fluxes from the tropical and subtropical oceans estimated by Andreae *et al.* (1985) and Ferek *et al.* (1986) and reflects the seasonal variability in the concentration of DMS in the surface waters of the North Pacific (Bates *et al.*, 1987). Consistent with the lower sea-to-air flux, the concentrations of DMS in the atmospheric mixed layer over the northeastern Pacific were also a factor of 3–5 lower than those measured over the tropical and subtropical oceans by Andreae *et al.* (1985) and Ferek *et al.* (1986).

*Methanesulfonic acid.* The vertical distribution of aerosol MSA is clearly related to that of its precursor compound, DMS (Figure 5), with highest values ( $0.2\text{--}0.3 \text{ nmol m}^{-3}$ ) in the mixed layer, and a decrease through the cloud convection layer into the free troposphere. Close to the sea surface, MSA is present in almost equal amounts within the coarse and fine particle mode, whereas in the free troposphere almost all MSA is in submicron particles. No aircraft measurements of MSA have been made before this study.

Our results from the mixed layer are comparable to the concentrations found by our group and by others at surface level in other temperate marine regions. At Cape Grim, Tasmania, which is in a climate zone similar to our measurement region, Ayers *et al.* (1986) found a mean MSA concentration of  $0.18 \text{ nmol m}^{-3}$  with a pronounced seasonal cycle (winter ca.  $0.05 \text{ nmol m}^{-3}$ , summer ca.  $0.5 \text{ nmol m}^{-3}$ ). At Shemya, in the Aleutian Islands and upwind of our flight region, Saltzman *et al.* (1986) observed a similarly pronounced seasonal cycle with a winter average of  $0.15 \text{ nmol m}^{-3}$  and a summer mean of  $1.8 \text{ nmol m}^{-3}$ . During a cruise in the temperate region of the North Atlantic during May 1984, we found a mean MSA concentration of  $0.49 \text{ nmol m}^{-3}$  (Church *et al.*, 1987). Our flights over the northeastern Pacific took place during the transition period from winter to spring/summer conditions in early May; the fact that our values are near the lower end of the range observed at Shemya supports our conclusion that the DMS levels in the northern North Pacific were still characteristic of winter conditions.

*Sulfur dioxide.* In contrast to the distributions of DMS and MSA, the  $\text{SO}_2$  profiles show an increase with altitude through the boundary layer (Figure 5).

This is in agreement with the assumption that the ocean is a sink for atmospheric  $\text{SO}_2$ . The concentrations measured in the mixed layer are substantially lower than previously reported average values for other ocean areas (Nguyen *et al.*, 1974, 1983; Bonsang *et al.*, 1980; Maroulis *et al.*, 1980; Herrmann and Jaeschke, 1984). However, they are consistent with the relatively low DMS concentrations discussed above, and probably reflect the low emission rate of biogenic sulfur from the ocean during winter and early spring. While the mean  $\text{SO}_2$  concentration reported by Nguyen *et al.* (1983) is about  $1.6 \text{ nmol m}^{-3}$ , close examination of their data shows that this average is strongly influenced by high values from upwelling areas and from the phytoplankton blooms in early summer in the Antarctic Convergence region. Their data from spring and fall show many values in the range of  $0.2\text{--}0.6 \text{ nmol m}^{-3}$ , close to our results.

There is a pronounced increase of the  $\text{SO}_2$  profiles either above the cloud tops (flights I and II) or at the cloud base level (flight II) which can be explained by the general subsidence and increasing stability of the atmosphere at these levels (Figures 3 and 4) and the advection of air masses which still had a continental 'imprint' in their chemical composition, as supported by the Rn and trajectory data.

The  $\text{SO}_2$  profiles from flights III and IV, which were conducted successively during the same day, show a maximum around 2–3 km and very low values at 4–6 km. This vertical distribution shows an inverse relationship to the relative humidity profile, which has a minimum around 3–4 km and a very pronounced maximum around 4–5 km (Figure 3). The low  $\text{SO}_2$  levels in this humid layer, in which regions of altocumulus were observed, are most likely explained by enhanced rates of conversion to sulfate by aqueous phase oxidation within cloud droplets. The fact that sulfate levels in this layer do not show a decrease comparable to  $\text{SO}_2$  is consistent with this explanation. The isentropic trajectories at 300 K, corresponding to this humidity maximum, show that the air had been in contact with the sea surface in the western North Pacific near Japan and had thereby taken up moisture, whereas the trajectories above or below this level do not contact the ocean surface within the preceding ten days.

*Nonsea-salt sulfate.* The vertical profiles of nonsea-salt sulfate ( $\text{nss-SO}_4^{2-}$ , Figure 5) show an increase in concentration from the boundary layer to the free troposphere, similar to the increase observed for  $\text{SO}_2$ . In the boundary layer, the  $\text{nss-SO}_4^{2-}$  concentrations were in the range of  $3\text{--}6 \text{ nmol m}^{-3}$ , similar to those observed at ground level at Cape Grim (Ayers *et al.*, 1986: mean  $2.8 \text{ nmol m}^{-3}$ ; Andreae, 1982: mean  $6.4 \text{ nmol m}^{-3}$ ). These results are also comparable to the concentrations measured at the island stations at Shemya ( $6.9 \text{ nmol m}^{-3}$ ) and Midway ( $3.2 \text{ nmol m}^{-3}$ ) during periods not influenced by Asian dust storms (Prospero *et al.*, 1985). The levels of  $\text{nss-SO}_4^{2-}$  in the free troposphere (*ca.*  $8 \text{ nmol m}^{-3}$ ) are higher than values found in the boundary layer; in fact, they exceed the levels observed in the uncontaminated marine boundary layer anywhere in the North Pacific (Prospero *et al.*, 1985), which suggests that sources

other than marine inputs are required to explain the abundance of  $\text{nss-SO}_4^{2-}$  in the free troposphere during our flights. The trajectory calculations (Figure 4) show contact with the Asian continent for most of the free troposphere levels sampled (above 2 km for flights I and II, above 3 km for flights III and IV), supporting the hypothesis that inputs from East Asia are responsible for the elevated  $\text{nss-SO}_4^{2-}$  levels. As mentioned above, the radon measurements are also consistent with air mass transport from Asia to our sampling area within about one week. During April/May 1979, Darzi and Winchester (1982) found similar concentrations of  $\text{nss-SO}_4^{2-}$  in the free troposphere at Mauna Loa Observatory, Hawaii, and related the elevated  $\text{nss-SO}_4^{2-}$  levels to Asian dust storm episodes.

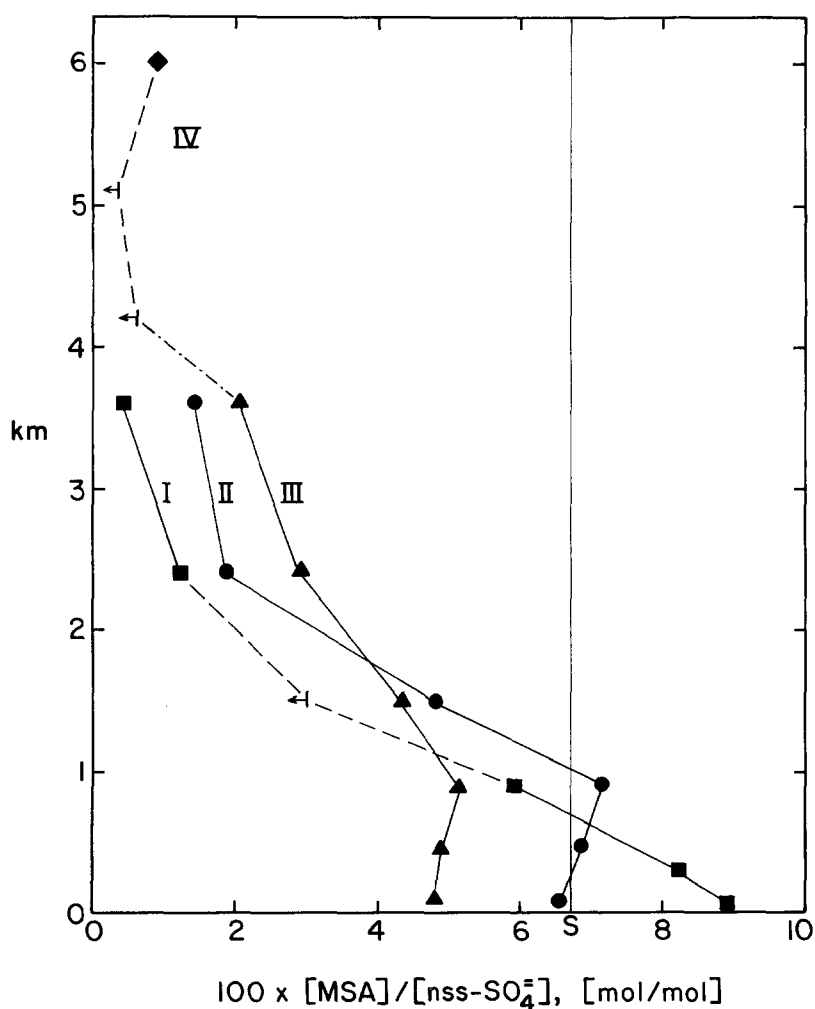


Fig. 6. Vertical distribution of the methanesulfonate/nonsea-salt sulfate mole ratio from flights I-IV. The vertical line labeled S shows the average for this ratio obtained by Saltzman *et al.* (1983) in the boundary layer over the Pacific Ocean.

On our flights, we did not measure any elements which could serve as tracers of Asian dust. We did, however, visually observe the presence of haze in the free troposphere during flight IV.

From surface level measurements at remote island stations, Saltzman *et al.* (1983, 1985) reported a strong correlation between  $\text{nss-SO}_4^{2-}$  and aerosol MSA concentrations which suggests a common biogenic source for both compounds within the marine environment. From their data they calculated an average value of 6.7% for the  $\text{MSA/nss-SO}_4^{2-}$  ratio in remote areas of the Pacific and Indian Oceans at sea level. In temperate regions this average is subject to seasonal variations, e.g., at Norfolk Island (29° S) it ranges from 2% during the cooler months to 12% during the warmer months. Ayers *et al.* (1986) found a mean value of 6.3% for this ratio at Cape Grim, also with a pronounced seasonal variation from about 2% in winter to ca. 18% in summer. Since aerosol MSA is very stable under atmospheric conditions, Saltzman *et al.* (1984) proposed that it may be used as a tracer for biogenic sulfur (particularly DMS) emissions. The  $\text{MSA/nss-SO}_4^{2-}$  ratio can thus help to discriminate between the biogenic and non-biogenic contribution to the  $\text{nss-sulfate}$  budget in the marine atmosphere if similar removal rates are assumed for both constituents. In Figure 6 we have plotted the vertical profiles of this ratio for flights I–IV. In the mixed layer, our data show ratios similar to those observed by Saltzman *et al.* (1983) and Ayers *et al.* (1986), whereas much lower values are found in the free troposphere, consistent with a transition from the dominance of biogenic to non-biogenic  $\text{nss-SO}_4^{2-}$  sources with altitude. The  $\text{MSA/nss-SO}_4^{2-}$  ratio shows a clear relationship to the concentration of DMS in the boundary layer, with the lowest values being found during flight III, which also had the lowest DMS concentrations. The values observed in the free troposphere over the North Pacific (ca. 1–2%) are similar to results we obtained in the mixed layer over the temperate North Atlantic when large amounts of anthropogenic sulfate from North America contributed to the sulfate aerosol (Church *et al.*, 1987). The largely non-biogenic origin of the  $\text{nss-SO}_4^{2-}$  in the free troposphere, together with the correlation between  $\text{nss-SO}_4^{2-}$  and  $\text{SO}_2$ , supports our previous conclusion that  $\text{SO}_2$  was predominantly of non-biogenic origin within the free troposphere.

*The sulfur cycle.* The vertical profiles of the individual sulfur species reflect the composite interactions of the exchange across the air/sea interface, local vertical transport and chemical reactions, and long-range advection into the sampling region. Vertical profiles of DMS similar to those described here, albeit at higher concentrations, have been observed in the tropics by Ferek *et al.* (1986) under conditions of low convective activity, and have been explained by these authors using a model incorporating chemical and transport processes. However, the steady-state assumption which could be reasonably made for tropical regions does not apply well to the conditions prevailing during our experiment. In the postfrontal situations which we had chosen for our flights, there is strong downward transport of free tropospheric air into the boundary layer, and

horizontal divergence at the surface level. Consequently, the air in the mixed layer cannot reach steady state with respect to processes which have time scales comparable to or longer than the boundary layer replacement time. This applies to the marine input of DMS, which has a time scale of about one half day based on the vertically integrated column content of DMS (*ca.*  $1 \mu\text{mol m}^{-2}$ ) and its sea-to-air flux (*ca.*  $2 \mu\text{mol m}^{-2} \text{d}^{-1}$ ), as well as to the conversion of DMS to MSA and  $\text{SO}_2$  (the lifetime of DMS relative to OH oxidation is *ca.* 36–48 h: Andreae *et al.*, 1985, and references therein).

It appears that postfrontal subsidence and the resulting atmospheric stability and suppressed vertical exchange were responsible for confining DMS largely to the mixed layer and for the pronounced concentration gradient from the mixed layer to the free troposphere. The low DMS concentrations observed during flight III coincide with the highest rate of subsidence into the boundary layer (Figure 4: May 11, 280 K) suggesting that under these conditions DMS had not yet had time to build up to the levels found during flights I and II. During flight III, we also found the highest  $\text{nss-SO}_4^{2-}$  levels and the lowest MSA/ $\text{nss-SO}_4^{2-}$  ratios in the boundary layer, which supports our hypothesis of significant introduction of free tropospheric air into the boundary layer during this period. The trajectories suggest that the subsiding free tropospheric air sampled below 2 km during flights I and II (Figure 4, 285K) had previous contact with the sea surface, which would explain the presence of MSA and  $\text{nss-SO}_4^{2-}$  at ratios typical of remote marine conditions.

In order to examine the relationships between the different sulfur compounds, we present a simple reservoir model (Figure 7), similar to the one given for tropical regions by Andreae (1986). In each box we show the column content of the species together with our best estimate of its residence time derived from the

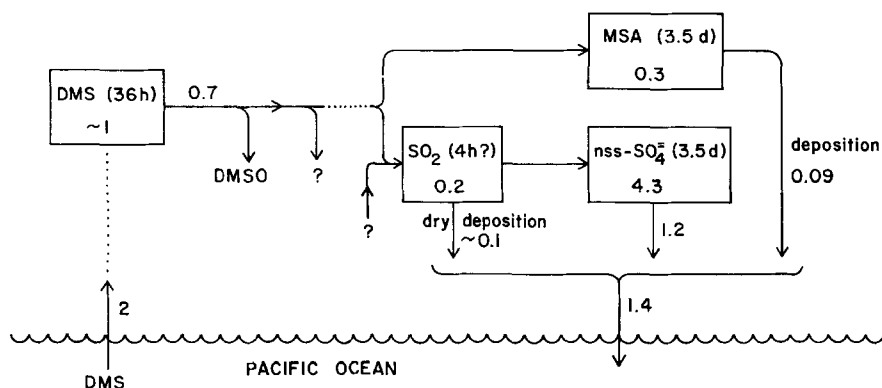


Fig. 7. Box model of the cycle of marine biogenic sulfur over the northeastern Pacific during the study period. Column-integrated concentrations are indicated inside the boxes in units of  $\mu\text{mol m}^{-2}$ , fluxes next to the arrows in units of  $\mu\text{mol m}^{-2} \text{d}^{-1}$ . The model has not been forced to a closed mass-balance; rather, the arrows indicate independent estimates of the fluxes through the individual boxes (see text).

literature. We have derived the marine biogenic component of  $\text{nss-SO}_4^{2-}$  from the MSA concentrations using a constant MSA/ $\text{nss-SO}_4^{2-}$  ratio of 6.7%. Examination of the fluxes in our model shows that the sea-to-air flux of DMS significantly exceeds the (column-integrated) oxidation rate of DMS by OH (2 vs.  $0.7 \mu\text{mol m}^{-2} \text{d}^{-1}$ ), suggesting that DMS has not yet reached a steady-state level. The deposition fluxes of MSA and the biogenic component of  $\text{nss-SO}_4^{2-}$  add up to  $1.3 \mu\text{mol m}^{-2} \text{d}^{-1}$ , which is reasonably consistent with a DMS input of  $2 \mu\text{mol m}^{-2} \text{d}^{-1}$ , especially considering that the deposition of other DMS oxidation products like  $\text{SO}_2$  and DMSO also contributes to the removal of DMS-derived sulfur. It is possible that at least part of the longer-lived MSA and  $\text{nss-SO}_4^{2-}$  aerosol is present as residual from the period when the air mass was previously in contact with the sea surface, and that these species may therefore be closer to steady state than DMS, for which all of the 'old' input has been oxidized during transport. The steady-state assumption leads to a very short lifetime for  $\text{SO}_2$ ; in order to support the  $\text{nss-SO}_4^{2-}$  deposition rate at the observed  $\text{SO}_2$  concentrations, we need a lifetime of  $\text{SO}_2$  with respect to oxidation to  $\text{SO}_4^{2-}$  of *ca.* 4 h (or less, if we assume a lifetime shorter than 3.5 days for the  $\text{nss-SO}_4^{2-}$  aerosol). Such short  $\text{SO}_2$  lifetimes imply that most  $\text{SO}_2$  oxidation takes place in the liquid phase (National Research Council, 1983, and references therein), which may be realistic in view of the fact that cumulus clouds were usually present in the boundary layer during our flights.

While it is clear that the complex situation and the nonsteady-state conditions prevailing during our flight experiment cannot be adequately described by such a simple model, this approach does help to identify the limitations of the steady-state assumption. It also suggests that the marine emission of DMS can account for most of the sulfur budget in the boundary layer. Comparison between the amounts of DMS-derived  $\text{nss-SO}_4^{2-}$  (about  $4\text{--}5 \mu\text{mol m}^{-2}$ , based on the MSA data) and the total column content of  $\text{nss-SO}_4^{2-}$  (*ca.*  $25 \mu\text{mol m}^{-2}$  to 6 km, flights III and IV), however, points to a predominantly continental origin for most of the  $\text{nss-SO}_4^{2-}$  in the troposphere during our experiment. Since the proportion of biogenic and non-biogenic  $\text{nss-SO}_4^{2-}$  shows a strong vertical gradient, the contribution of these two components to sulfate deposition depends strongly on cloud physical processes and cannot be easily predicted from our data.

### 3.4. Sodium, Ammonium, and Nitrate

The vertical distributions of  $\text{Na}^+$  (Figure 8) provide direct information about the mixing height of the sea-salt aerosol. As expected, we found  $\text{Na}^+$  to be almost exclusively present within the coarse particle mode. A significant decrease in the  $\text{Na}^+$  concentration was observed during flights II and III above 1 km, which coincided with the cloud base level. The  $\text{Na}^+$  profile obtained during flight I shows a strong inversion at a level of 0.3 km. The occurrence of such sea-salt

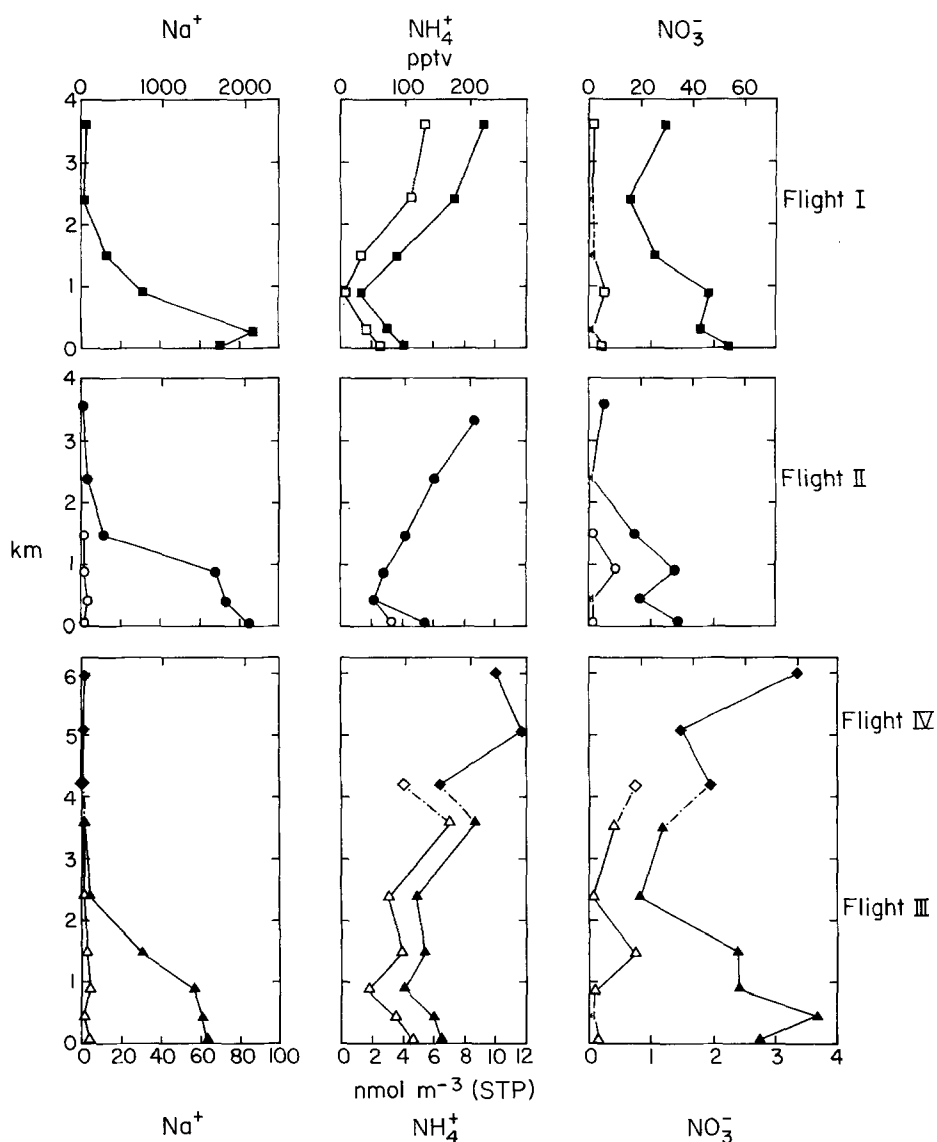


Fig. 8. Vertical distributions of sodium ( $\text{Na}^+$ ), ammonium ( $\text{NH}_4^+$ ), and nitrate ( $\text{NO}_3^-$ ) aerosol measured over the northeastern Pacific during flights I-IV (3-11 May 1985). The open symbols represent the fraction below  $1.5 \mu\text{m}$  diameter and the closed symbols the total concentration.

inversion layers, typically between 0.3–0.6 km altitude, has been observed earlier by Blanchard (1983) and Blanchard and Woodcock (1980). Accordingly the maximum in the  $\text{Na}^+$  profile measured during flight I may have been related to the low altitude of the cloud base level where the relative humidity was 80%, while it was about 75% (the deliquescence point of  $\text{NaCl}$ ) within the inversion layer (Figure 3). Thus hygroscopic sea-salt particles which grow and shrink in

size as a function of the relative humidity could have accumulated within this layer due to an equilibrium between updraft and settling velocities. Such conditions were especially favored on the first flight day.

In contrast to the sodium distributions, the  $\text{NH}_4^+$  profiles shown in Figure 8 reflect the distribution of the nonsea-salt portion of the marine aerosol throughout most of the vertical column. In the marine boundary layer, however, the highest  $\text{NH}_4^+$  concentrations were always measured within the lowest flight levels. Also, at least for these levels, all mass distributions given in Figure 8 show an appreciable amount of  $\text{NH}_4^+$  occurring in particles larger than  $1\ \mu\text{m}$  diameter, although it is generally predominant within the fine particle mode of the marine aerosol. These results may thus suggest a small but significant flux of ammonia from the ocean to the atmosphere which contributes to the ammonium ion levels in the boundary layer aerosol. At higher altitudes, however,  $\text{NH}_4^+$  is probably a good tracer for the extent of advection and downward mixing of air masses due to postfrontal subsidence.

Figure 9 shows the profiles of the  $\text{NH}_4^+/\text{nss-SO}_4^{2-}$  mole ratio for flights I–IV. With few exceptions, this ratio is between 1 and 2 at all altitudes, corresponding to an aerosol composition between  $(\text{NH}_4)_2\text{SO}_4$  and  $(\text{NH}_4)\text{HSO}_4$ . In the mixed layer the mean ratio is  $1.0 \pm 0.3$ , in the free troposphere it is  $1.4 \pm 0.2$ . This composition range is consistent with the observed dependence of the size distribution of the  $\text{nss-SO}_4^{2-}$  component on relative humidity (Figure 10): our data show a continuous increase in the relative amount of  $\text{nss-SO}_4^{2-}$  in the coarse aerosol fraction with humidity, as would be predicted from the laboratory growth curves for aerosols with  $\text{NH}_4^+/\text{SO}_4^{2-}$  ratios of 1.4 and lower (Tang 1980; the small jumps in the growth curves seen in the laboratory studies near 40 and 67% RH cannot be resolved in our field data).

The  $\text{NO}_3^-$  profiles obtained during flights I–IV (Figure 8) show that nitrate is predominantly present in the coarse particle mode at all altitudes. In the marine boundary layer, this is readily explained by the reaction of gaseous nitric acid with sea-salt particles leading to nitrate formation and appreciable loss of chloride due to the production and volatilization of HCl. Similar processes may have occurred in the particles of continental origin which were dominant in the upper flight levels. All measurements showed  $\text{Cl}^-$  enrichment factors of 0.87–1.0 within the coarse particle mode. Klockow *et al.* (1979) have demonstrated that the reaction described above may lead to an appreciable enrichment of nitrate on filters during aerosol sampling. In fact it may even be used to trap gaseous  $\text{HNO}_3$  quantitatively on a NaCl-impregnated filter (e.g., Appel *et al.*, 1980). With respect to our measurements, however, we consider this effect to be insignificant due to the very low loading on the filters and the short sampling time of only 30 minutes within the boundary layer. Using virtual impactors, Savoie and Prospero (1982) have also shown that most of the large-particle nitrate is already present in the atmosphere and is not a sampling artifact.

The nitrate levels observed in the boundary layer ( $1.4\text{--}3.6\ \text{nmol m}^{-3}$ ) are

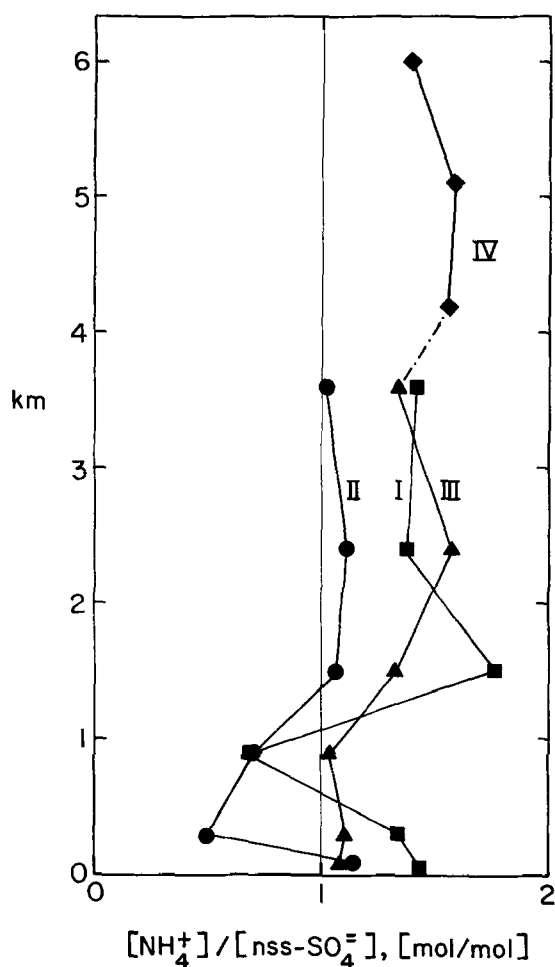


Fig. 9. Vertical distribution of the ammonium/nonsea-salt sulfate mole ratio from flights I-IV.

similar to the surface data from the SEAREX network: Prospero *et al.* (1985) give a range of 2.9–5.6 nmol m<sup>-3</sup> for the means of their North Pacific stations and a mean value of 1.6 nmol m<sup>-3</sup> for the South Pacific. On the GAMETAG flights, Huebert and Lazrus (1980) found nitrate concentrations of 2 and 4 nmol m<sup>-3</sup> in the Southern and Northern Hemisphere marine boundary layers, respectively – again in excellent agreement with our data. Our values from the free troposphere, 1–3.5 nmol m<sup>-3</sup>, also agree with the GAMETAG results (average *ca.* 2 nmol m<sup>-3</sup>). This agreement between our data and the GAMETAG values suggests that our sampling system did not collect significant amounts of gaseous HNO<sub>3</sub> on the aerosol filters. Our nitrate concentrations are also consistent with the total nitrate (HNO<sub>3</sub> + NO<sub>3</sub>) levels predicted by the two-dimensional model of Crutzen and Gidel (1983).

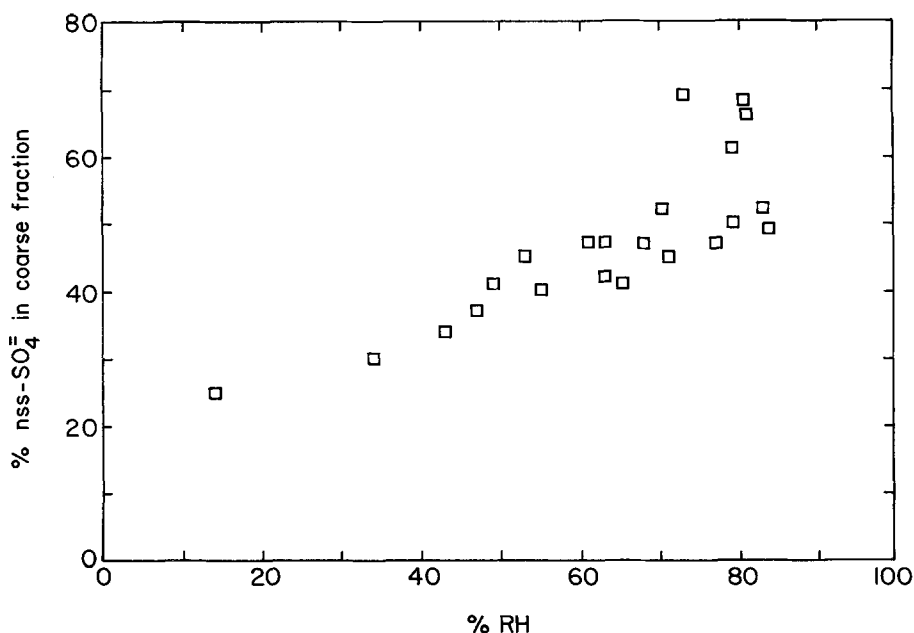


Fig. 10. Percentage of nonsea-salt sulfate observed in the coarse ( $> 1.5 \mu\text{m}$  diameter) fraction of the aerosol as a function of relative humidity.

The nitrate profiles show the presence of a minimum in the 2–3 km region and an inversion near cloud base which is most pronounced in the fine particle mode. The elevated nitrate concentrations in the boundary layer could be related to an enhanced rate of conversion of nitrogen oxides to nitrate, or to an increase in the amount of aerosol nitrate by transfer of gaseous  $\text{HNO}_3$  to the condensed phase. In view of the presence of convective cloud in the boundary layer and the fact that the increase of nitrate by *ca.*  $1\text{--}2 \text{ nmol m}^{-3}$  from 2 km to the surface corresponds to the conversion of only about 20–50 ppt  $\text{NO}_x$ , both mechanisms must be considered feasible under the conditions of our experiment. The recent observation of substantial amounts of amino acids in marine rain (Mopper and Zika, 1987) suggest an additional mechanism for the formation of nitrate in the marine boundary layer. Since these amino acids appear to originate from the sea surface, they would be present in the sea-salt aerosol, where they would yield nitrate as a product of photochemical decomposition. Experiments in which all pertinent nitrogen species are measured will be needed to resolve this question.

#### 4. Summary and Conclusions

- DMS concentrations both in seawater and in the atmospheric boundary layer were significantly lower than values previously reported for subtropical and

tropical regions, reflecting the seasonal variability of DMS production in the temperate North Pacific. Elevated DMS concentrations were found in coastal areas.

- The vertical profiles of DMS, MSA,  $\text{SO}_2$ , and  $\text{nss-SO}_4^{2-}$  were found to be strongly dependent on the convective stability of the atmosphere and on air mass origin. DMS and aerosol MSA both showed a similar decrease with altitude, consistent with the production of MSA from the photochemical oxidation of DMS. In contrast to the vertical distribution of DMS and MSA, a steady increase in  $\text{SO}_2$  concentration with altitude was generally observed. Nonsea-salt sulfate decreased with height in the marine boundary layer and increased sharply in the free troposphere where it showed a close correlation with  $\text{SO}_2$ .
- While biogenic sulfur emissions could account for most of the sulfur budget in the boundary layer, long-range transport of continentally derived air masses was mainly responsible for the elevated levels of both  $\text{SO}_2$  and  $\text{nss-SO}_4^{2-}$  in the free troposphere. This conclusion is supported by isentropic trajectories and radon measurements, which both suggest substantial transport from Asia with transit times of 4–8 days.
- $\text{NH}_4^+$  and  $\text{nss-SO}_4^{2-}$  showed a strong correlation; their molar ratio was generally between 1 and 2. The particle size distribution of this ammonium bisulfate/sulfate aerosol varied with relative humidity in agreement with theoretical predictions. A sea-to-air flux of ammonia is suggested by upward  $\text{NH}_4^+$  concentration gradients observed close to the sea surface. MSA was almost equally distributed in mass between fine and coarse mode particles in the mixed layer, but was predominantly in the submicron size range at higher altitudes. Nitrate was predominantly found in coarse particles, which also showed a chloride deficit relative to sea-salt composition, presumably due to surface reactions with gaseous nitric acid.
- We conclude from our results that long-range transport of atmospheric pollutants, in particular oxides of nitrogen and sulfur, makes an important contribution to the chemistry of the atmosphere in this 'remote' region. This is not evident in our boundary layer measurements which are very similar to data from uncontaminated regions, e.g., the southern hemisphere oceans, but is quite clear from the measurements in the free troposphere. Since surface measurements in remote regions may not show evidence of mid-tropospheric transport processes, as documented in this study, they are only of limited value for the assessment of the role of long-range transport of anthropogenic pollutants.

## Acknowledgements

We would like to thank the pilots of the NCAR 'King Air' and the staff of the NCAR Research Aviation Facility for their extensive cooperation. MOA

acknowledges support from NCAR during his sabbatical in spring 1985 and would like to thank R. Cicerone for the invitation to come to NCAR. We are grateful for the technical support of the NCAR machine shop during the construction of the aircraft sampling equipment. A. C. Delany provided numerous valuable suggestions for the design of the aerosol sampling system. We are also indebted to W. Zoller for use of his laboratory and ion chromatograph facilities at the University of Washington, and to S. Kelly-Hansen and M. Strom for their assistance with analysis of DMS in seawater. MAK gives particular thanks to Dennis Knowlton and Bill Dawson, and acknowledges helpful discussions and advice from R. E. Larson and J.-C. Leroulet (who also supplied calibrated filter standards) and the able assistance of Stefan Rosner, Tom Johns, and Michael Nguyen. R. Platner assisted with the trajectory analysis. We thank M. Dancy for help with the preparation of the manuscript and figures. This work was supported by the National Science Foundation (ATM-8407137) and by the National Oceanic and Atmospheric Administration under the National Acid Precipitation Assessment Program. Support for the radon measurements was provided by the Earth Science and Applications Division and the Biological Research Branch of the National Aeronautics and Space Administration under Joint Research Interchanges NCA-OR748-301 and NCA-OR748-302. The trajectory calculations were done using NSF-supported computer facilities at the National Center for Atmospheric Research.

## References

- Andreae, M. O., 1982, Marine aerosol chemistry at Cape Grim, Tasmania and Townsville, Queensland, *J. Geophys. Res.* **87**, 8875–8885.
- Andreae, M. O., 1985, The emission of sulfur to the remote atmosphere, in J. N. Galloway, R. J. Charlson, M. O. Andreae, and H. Rodhe (eds.), *The Biogeochemical Cycling of Sulfur and Nitrogen in the Remote Atmosphere*, D. Reidel, Dordrecht, pp. 5–25.
- Andreae, M. O., 1986, The ocean as a source of atmospheric sulfur compounds, in P. Buat-Ménard (ed.), *The Role of Air-Sea Exchange in Geochemical Cycling*, D. Reidel, Dordrecht, pp. 331–362.
- Andreae, M. O. and Raemdonck, H., 1983, Dimethylsulfide in the surface ocean and the marine atmosphere: a global view, *Science* **221**, 744–747.
- Andreae, M. O., Ferek, R. J., Bermond, F., Byrd, K. P., Engstrom, R. T., Hardin, S., Houmère, P. D., LeMarrec, F., Raemdonck, H., and Chatfield, R. B., 1985, Dimethylsulfide in the marine atmosphere, *J. Geophys. Res.* **90**, 12,891–12,900.
- Appel, B. R., Wall, S. M., Tokiwa, Y., and Haik, M., 1980, Simultaneous nitric acid, particulate nitrate and acidity measurements in ambient air, *Atmos. Environ.* **14**, 549–554.
- Atkinson, R. J., Pitts, J. N. Jr., and Aschmann, S. M., 1984, Tropospheric reactions of dimethyl sulfide with  $\text{NO}_3$  and OH radicals, *J. Phys. Chem.* **88**, 1584–1587.
- Ayers, G. P., Ivey, J. P., and Goodman, H. S., 1986, Sulfate and methanesulfonate in the maritime aerosol at Cape Grim, Tasmania, *J. Atmos. Chem.* **4**, 173–185.
- Bates, T. S. and Cline, J. D., 1985, The role of the ocean in a regional sulfur cycle, *J. Geophys. Res.* **90**, 9168–9172.
- Bates, T. S., Cline, J. D., Gammon, R. H., and Kelly-Hansen, S. R., 1987, Regional and seasonal variations in the flux of oceanic dimethylsulfide to the atmosphere, *J. Geophys. Res.* **92**, 2930–2938.
- Blanchard, D. C., 1983, The production, distribution, and bacterial enrichment of the sea-salt

- aerosol, in P. S. Liss and W. G. N. Slinn (eds.), *Air-Sea Exchange of Gases and Particles*, D. Reidel, Dordrecht, pp. 407–454.
- Blanchard, D. C. and Woodcock, A. H., 1980, The production, concentration, and vertical distribution of the sea-salt aerosol, *Annals New York Acad. Sci.* **338**, 330–347.
- Bonsang, B., Nguyen, B. C., Gaudry, A., and Lambert, G., 1980, Sulfate enrichment in marine aerosols owing to biogenic gaseous sulfur compounds, *J. Geophys. Res.* **85**, 7410–7416.
- Church, T. M., Tramontano, J. M., Whelpdale, D. M., Andreae, M. O., Galloway, J. N., Keene, W. C., Knap, A. H., and Tokos, J., 1987, Atmospheric and precipitation chemistry over the North Atlantic Ocean; shipboard results from April–May 1984, *J. Geophys. Res.*, to be submitted.
- Crutzen, P. J. and Gidel, L. T., 1983, A two-dimensional photochemical model of the atmosphere. 2: The tropospheric budgets of the anthropogenic chlorocarbons CO, CH<sub>4</sub>, CH<sub>3</sub>Cl and the effect of various NO<sub>x</sub> sources on tropospheric ozone, *J. Geophys. Res.* **88**, 6641–6661.
- Darzi, M. and Winchester, J. W., 1982, Aerosol characteristics at Mauna Loa Observatory, Hawaii, after East Asian dust storm episodes, *J. Geophys. Res.* **87**, 1251–1258.
- Daum, P. H. and Leahy, D. F., 1983, *The Brookhaven National Laboratory Filter Pack System for Collection and Determination of Air Pollutants*, Brookhaven National Lab., Upton, NY, Informal Report BNL 31381R.
- Evans, R. G., 1955, *The Atomic Nucleus*, McGraw-Hill, New York.
- Ferek, R. J., Chatfield, R. B., and Andreae M. O., 1986, Vertical distribution of dimethylsulfide in the marine atmosphere, *Nature* **320**, 514–516.
- Grosjean, D., 1984, Photooxidation of methyl sulfide, ethyl sulfide, and methanethiol, *Environ. Sci. Technol.* **18**, 460–468.
- Hatakeyama, S., Izumi, K., and Akimoto, H., 1985, Yield of SO<sub>2</sub> and formation of aerosol in the photo-oxidation of DMS under atmospheric conditions, *Atmos. Environ.* **19**, 135–141.
- Herrmann, J. and Jaeschke, W., 1984, Measurements of H<sub>2</sub>S and SO<sub>2</sub> over the Atlantic Ocean, *J. Atmos. Chem.* **1**, 111–123.
- Holmén, K. and Liss, P., 1984, Models for air-water gas transfer: an experimental investigation, *Tellus* **36B**, 92–100.
- Huebert, B. J. and Lazrus, A. L., 1980, Tropospheric gas-phase and particulate nitrate measurements, *J. Geophys. Res.* **85**, 7322–7328.
- John, W., Hering, S., Reischl, G., Sasaki, G., and Goren, S., 1983, Characteristics of Nuclepore filters with large pore size – II. Filtration properties, *Atmos. Environ.* **17**, 373–382.
- Klockow, D., Jablonski, B., and Niessner, R., 1979, Possible artifacts in filter sampling of atmospheric sulphuric acid and acidic sulphates, *Atmos. Environ.* **13**, 1665–1676.
- Kritz, M. A., 1982, Exchange of sulfur between the free troposphere, marine boundary layer and the sea surface, *J. Geophys. Res.* **87**, 8795–8803.
- Küchemann, D. and Weber, J., 1953, *Aerodynamics of Propulsion*, McGraw-Hill, New York.
- Larson, R. E., 1973, Measurements of radioactive aerosol using thin plastic scintillators, *Nucl. Instr. Meth.* **108**, 467–470.
- Liu, S. C., McAfee, J. R., and Cicerone, R. J., 1984, Radon 222 and tropospheric vertical transport, *J. Geophys. Res.* **89**, 7291–7297.
- McLeod, H., Jourdain, J. L., Poulet, G., and Le Bras, G., 1984, Kinetic study of reactions of some organic sulfur compounds with OH radicals, *Atmos. Environ.* **18**, 2621–2626.
- Maroulis, P. J., Torres, A. L., Goldberg, A. B., and Bandy, A. R., 1980, Atmospheric SO<sub>2</sub> measurements on project GAMETAG, *J. Geophys. Res.* **85**, 7345–7349.
- Merrill, J. T., Bleck, R., and Avila, L., 1985, Modeling atmospheric transport to the Marshall Islands, *J. Geophys. Res.* **90**, 12,927–12,936.
- Mopper, K. and Zika, R. G., 1986, Free amino acids in marine rains: evidence for oxidation and potential role in nitrogen cycling, *Nature* **325**, 246–249.
- National Research Council, 1983, *Acid Deposition: Atmospheric Processes in Eastern North America*, National Academy Press, Washington, D.C.
- Nguyen, B. C., Bonsang, B., and Lambert, G., 1974, The atmospheric concentration of sulfur dioxide and sulfate aerosols over antarctic, subantarctic areas and oceans, *Tellus* **26**, 241–249.
- Nguyen, B. C., Bonsang, B., and Gaudry, A., 1983, The role of the ocean in the global atmospheric sulfur cycle, *J. Geophys. Res.* **88**, 10,903–10,914.

- Niki, H., Maker, P. D., Savage, C. M., and Breitenbach, L. P., 1983, An FTIR study of the mechanism of the reaction  $\text{HO} + \text{CH}_3\text{SCH}_3$ , *Int. J. Chem. Kinet.* **15**, 647–654.
- Parsons, T. R., Maita, Y., and Lalli, C. M., 1984, *A Manual of Chemical and Biological Methods for Seawater Analysis*, Pergamon Press, New York, 173 p.
- Polian, G., 1972, Mesures de la radioactivité atmosphérique naturelle par appareils alpha semi-automatiques. Report, CNRS, Gif-sur-Yvette, France.
- Prospero, J. M., Savoie, D. L., Nees, R. T., Duce, R. A., and Merrill, J., 1985, Particulate sulfate and nitrate in the boundary layer over the North Pacific Ocean, *J. Geophys. Res.* **90**, 10,586–10,596.
- Saltzman, E. S., Gidel, L. T., Zika, R. G., Milne, P. J., Prospero, J. M., Savoie, D. L., and Cooper, W. J., 1984, Aerosol chemistry of methane sulfonic acid, in L. Newman (ed.), *Gas-Liquid Chemistry of Natural Waters*, Brookhaven National Laboratory, Upton, NY, Report BNL 51757, pp. 53/1–8.
- Saltzman, E. S., Savoie, D. L., Prospero, J. M., and Zika, R. G., 1985, Atmospheric methanesulfonic acid and non-sea-salt sulfate at Fanning and American Samoa, *Geophys. Res. Lett.* **12**, 437–440.
- Saltzman, E. S., Savoie, D. L., Prospero, J. M., and Zika, R. G., 1986, Methanesulfonic acid and non-sea-salt sulfate in Pacific air: regional and seasonal variations, *J. Atmos. Chem.* **4**, 227–240.
- Saltzman, E. S., Savoie, D. L., Zika, R. G., and Prospero, J. M., 1983, Methane sulfonic acid in the marine atmosphere, *J. Geophys. Res.* **88**, 10,897–10,902.
- Savoie, D. L., and Prospero, J. M., 1982, Particle size distribution of nitrate and sulfate in the marine atmosphere, *Geophys. Res. Lett.* **9**, 1207–1210.
- Talbot, R. W., Andreae, M. O., Andreae, T. W., and Harriss, R. C., 1987, Regional aerosol chemistry of the Amazon Basin, *J. Geophys. Res.*, in press.
- Tang, I. N., 1980, Deliquescence properties and particle size changes of hygroscopic aerosols, in K. Willeke (ed.), *Generation of Aerosols*, Ann Arbor Science Publishers, Ann Arbor, MI.
- Van Valin, C. C. and Luria, M., 1985,  $\text{O}_3$ , CO, hydrocarbons and dimethyl sulfide over the western Atlantic Ocean, *Eos* **66**, 833.
- Wilkniss, P. E., Lamontagne, R. A., Larson, R. E., Swinnerton, J. R., Dickson, C. R., and Thompson, T., 1973, Atmospheric trace gases in the southern hemisphere, *Nature Physical Science* **245**, 45–47.
- Wine, P. H., Kreutter, N. M., Grump, C. A., and Ravishankara, A. R., 1981, Kinetics of OH reactions with the atmospheric sulfur compounds  $\text{H}_2\text{S}$ ,  $\text{CH}_3\text{SH}$ ,  $\text{CH}_3\text{SCH}_3$  and  $\text{CH}_3\text{SSCH}_3$ , *J. Phys. Chem.* **85**, 2660–2665.
- Winer, A. M., Atkinson, R., and Pitts, J. N. Jr., 1984, Gaseous nitrate radical: possible nighttime atmospheric sink for biogenic organic compounds, *Science* **224**, 156–159.